

# SVV\_A05.pdf

*by* Nick Pauly

---

**Submission date:** 01-Mar-2019 05:02PM (UTC+0100)

**Submission ID:** 1086029854

**File name:** SVV\_A05.pdf

**Word count:** 11623

**Character count:** 52989

# Technical report

---

AE3212-II Simulation, Verification and Validation

BSc Aerospace engineering

Group A05

4550447 Nick Pauly  
4303067 Willem Volker  
4530802 Andreas Biront  
4588304 Reinier Vos  
4551575 Angela Hekker  
4569431 Luc Boerboom

# Contents

1

<b>1</b>	<b>Introduction</b>	<b>1</b>
<b>2</b>	<b>Problem analysis</b>	<b>2</b>
2.1	General assumptions . . . . .	2
2.2	Input and output data . . . . .	3
<b>3</b>	<b>Analytical model</b>	<b>4</b>
3.1	Assumptions . . . . .	4
3.2	Geometrical properties . . . . .	4
3.3	Bending . . . . .	5
3.4	Torsion . . . . .	5
<b>4</b>	<b>Numerical model</b>	<b>6</b>
4.1	Reference frame . . . . .	6
4.2	Structural idealization and assumptions . . . . .	6
4.3	Cross-sectional properties . . . . .	7
4.4	Reaction forces . . . . .	8
4.5	Torsion . . . . .	12
4.6	Shear flows and Deflection . . . . .	13
4.7	Computational model . . . . .	14
<b>5</b>	<b>Verification</b>	<b>17</b>
5.1	Code verification and Calculation Verification . . . . .	17
5.2	Comparison . . . . .	18
<b>6</b>	<b>Validation</b>	<b>22</b>
6.1	Assumptions . . . . .	22
6.2	Experimental Data Description . . . . .	22
6.3	Data transformation . . . . .	22
6.4	Comparison . . . . .	23
<b>7</b>	<b>Conclusion</b>	<b>24</b>
<b>Bibliography</b>		<b>25</b>
<b>Appendix</b>		<b>25</b>

# 1 Introduction



The ailerons of an aircraft enable the pilot to roll the aircraft, and are thus a vital component in steering the aircraft. Therefore, it is crucial to know the effects of loads imposed on the aileron on the deflection of the structure and the stresses that occur within it. To this end, it is necessary to test the structure of the aileron, however these tests tend to be expensive and time consuming. An alternative way of approximating the aileron deflections and stresses is by setting up a numerical model, which simulates the aileron structure when enduring the loads that occur during flight.

The purpose of this report is to describe the development of a numerical model of an aileron on the Airbus A320, as well as the verification and validation of said model. Verification is done using an analytical model, while validation is performed using data obtained from a finite element method (FEM).

To be more specific, this project aims to answer the following questions:

- What is the deflection of the leading and trailing edge of the aileron?
- What is the shear stress in each rib?
- What is the maximum shear flow in the ribs?
- Does the numerical model provide a correct result?
- How accurate is the numerical model?

This report is structured as follows: all general information regarding the problem can be found in chapter 2. Information on the analytical model is given in chapter 3. The numerical model is described in chapter 4. Verification and validation of the numerical model are performed in chapter 5 and chapter 6, respectively. Finally, chapter 7 provides the conclusion.

## 2 Problem analysis

This chapter covers the basic information needed to solve the problem. In section 2.1 the general assumptions are explained, as well as their impact on the calculations done to solve the problem. Then, section 2.2 shows all the input data needed to do the calculations as well as the output data that will be calculated.

### 2.1 General assumptions

Listed below are all general assumptions, which apply to both the numerical and the analytical model. With each assumption, the estimated effects on the results are described.

- **The material is homogeneous and isotropic:** The aileron is made out of aluminium 2024-T3, which is assumed to have the same properties throughout the entire aileron in every direction. This assumption is not expected to have a very significant impact on the results of the model, as material imperfections are assumed to be small, rare, and somewhat evenly distributed over the structure.
- **The cross-section of the aileron is constant in x direction:** the cutouts in the leading edge of the aileron due to the hinges and actuators are neglected. Due to this, the structure might appear stronger than it really is, and calculated deformations might be smaller than they would be in reality. In addition, possible stress concentrations at the leading edge cutouts are not accounted for.
- **The net aerodynamic load acts as a uniformly distributed load q:** the aileron has a constant profile and chord length and thus the aerodynamic load working on it can be assumed to be uniform.
- **Aileron weight can be neglected:** compared to the other forces working on the aileron, its own weight can be considered negligible. This can be shown by doing a simple calculation: the given analytical model shows the total cross-sectional area of the aileron to be  $2743\text{mm}^2$ . Multiplying this value with the aileron length of  $2771\text{mm}$ , the material density of  $2780\text{kg/m}^3$ [1] and the gravitational constant g of  $9.81\text{m/s}^2$  will result in an approximation of the aileron weight:

$$\text{Eq 4} \quad \frac{2743 * 2771}{10^9} * 2780 * 9.81 = 207.3\text{N}$$

Clearly, this is much smaller than the forces working on the aileron, which are orders of magnitude larger as can be seen in Figure 2.1. Therefore, this assumption is not expected to have much of an impact on the results.

- **The aileron can be modelled as a beam:** This assumption implies that the deflection of the beam is negligible with respect to its length, which simplifies modelling greatly. It will be assumed that all loadings continue to act with the same orientation, even when deflection or twist occurs in the aileron structure.
- **The reaction loads at the hinges and actuators can be modelled as points loads:** In reality, these loads would be distributed, however the areas on which they act are small compared to the aileron. Therefore they will be considered point loads instead of distributed loads. This assumption will have an impact on when the shear is calculated near the point load.

- The hinges only restrict translations but allow rotations: the hinges provide reaction forces, however they allow the aileron to rotate around one axis, and thus do not provide a reaction moment around this axis.
- Attachments of the stiffeners to the skin of the aileron do not have to be analysed: Stresses due to these attachments are neglected, which could result in an overestimation of the strength of the aileron. However, this effect is expected to be small due to the small dimensions of the attachments with respect to the aileron dimensions.

## 2.2 Input and output data

This section gives an overview of the input data needed during the calculations and the output that will be calculated. The input data is used to compute the maximum deflection of the leading and trailing edge. These calculations are needed to see how the aileron works under aerodynamic forces. Maximum shear flow in the ribs of the aileron will also be computed to see if the aileron will endure the forces during flight. All input data needed for the calculations are represented in Figure 2.1. Table 2.1 shows the output data to be calculated.

Property	Symbol	Value	Unit
Chord length aileron	$C_a$	0.547	m
Span of the aileron	$l_a$	2.771	m
x-location of hinge 1	$x_1$	0.153	m
x-location of hinge 2	$x_2$	1.281	m
x-location of hinge 3	$x_3$	2.681	m
Distance between actuator 1 and 2	$x_a$	28.0	cm
Aileron height	$h$	22.5	cm
Skin thickness	$t_{sk}$	1.1	mm
Spar thickness	$t_{sp}$	2.9	mm
Thickness of stiffener	$t_{st}$	1.2	mm
Height of stiffener	$h_{st}$	1.5	cm
Width of stiffener	$w_{st}$	2.0	cm
Number of stiffeners (equally spaced along the periphery of the cross-section)	$n_{st}$	17	-
Vertical displacement hinge 1	$d_1$	1.103	cm
Vertical displacement hinge 3	$d_3$	1.642	cm
Maximum upward deflection	$\theta$	26	deg
Load in actuator 2	P	91.7	kN
Net aerodynamic load	q	4.53	kN/m

Figure 2.1: Input data 

Property	Symbol	Unit
Maximum deflection of the leading edge	$\delta_{LE,max}$	m
Maximum deflection of the trailing edge	$\delta_{TE,max}$	m
Maximum shear flow in rib A	$q_{A,max}$	N/m
Maximum shear flow in rib B	$q_{B,max}$	N/m
Maximum shear flow in rib C	$q_{C,max}$	N/m
Maximum shear flow in rib D	$q_{D,max}$	N/m

Table 2.1: Output data

## 3 Analytical model

[ 7 ]

This chapter will describe the analytical model and how it would help improve the results that are given by the numerical model. The assumptions and their effects are described in section 3.1. The analytical model works as follows: all relevant geometrical properties are calculated first, after which all separate load cases are analyzed. Finally, all load cases are superimposed to give the final results on the reaction forces and displacements of the aileron leading and trailing edge on a discrete number of points. The model does not provide direct values for the shear flow in the structure.

### 3.1 Assumptions

[ 8 ]

Listed below are the assumptions which are applicable to the analytical model. These assumptions were retrieved from the provided model description, as well as things that were noticed while using the model.

[ 15 ]

- **Aileron is thin-walled:** the thin-walled approximation can be made when the radius of a structure is at least an order of magnitude larger than the thickness of its walls. If this is the case, the thin-walled approximation allows to neglect all higher orders of the wall thickness  $t$  ( $t^2, t^3$ , etc.) in any subsequent calculations. This assumption holds for both the skin walls (1.1 mm), as well as for the slightly thicker spar wall (2.9 mm).
- **The analysis for shear forces and for torsion are decoupled:** Three load cases are considered and superimposed in this model: bending due to boundary conditions, bending due to loading, and torsion. By considering these load cases separately, it is assumed that deformations due to each loading case are sufficiently small that they do not influence other loading cases and [ 9 ] their effects on the structure. This means that each loading case can be considered individually first, and they can then be superimposed to arrive at the final deformation and stress state. Due to the fact that for each load case, the deformations have indeed been shown to be very small, this assumption is not expected to have a very large impact on the results.
- **Centroid on hingeline:** In the analytical model, it seems that it was assumed that the centroid is located at the coordinate origin, which is located in the hinge line. This appears from the fact [ 10 ] that the given  $d_y$  used for coordinating the Steiner terms for each component, is the distance from the hinge line to the centroid of the given component. Using the given data regarding component locations and areas, the actual centroid was calculated and estimated to be over 100 mm away from the hinge line. The use of the hinge line as centroid causes  $I_{yy}$  to be much larger than the value found with the numerical method, but has no effect on  $I_{zz}$ , as the centroid is at  $y=0$  in both methods. The mistake was corrected by taking the newly calculated centroid, re-calculating the Steiner terms and adding them to the  $I_{yy}$  of each component about its own centroid. [ 11 ] This resulted in a large decrease in moment of inertia, and a much more similar value to the one calculated using the numerical model.

### 3.2 Geometrical properties

[ 12 ]

For analysis of the geometrical properties, the aileron cross-section is split up into 21 parts: 17 stiffeners, evenly distributed over the aileron circumference; the lower and upper skin; the spar and the leading edge. The total moment of inertia is the sum of the moment of inertia of each component about its own centroid, and the Steiner term of each component. For the stiffeners, not only their

location but also their orientation is taken into account, as they are placed under a certain inclination with respect to the frame of reference.

The torsional rigidity J is calculated by using the equation for a thin-walled multicell cross-section:

$$J = \frac{4A^2}{\oint \frac{ds}{t}} \quad (3.1)$$

Where A is the total area enclosed by the cross-section, and  $\oint$  is the integration of the total wall length. Considering that the wall thickness t is not constant, the factor  $\frac{ds}{t}$  must be considered per section.

### 3.3 Bending

Bending in the aileron occurs due to both boundary conditions (a forced displacement of hinges 1 and 3), as well as due to loading that is imposed on the structure. In the analytical model, all forces which do not yet act on the hinge line, i.e. the distributed load q and both actuator forces P and  $P_R$ , are moved to the hinge line. The torques that now act on the structure due to this, are taken into account when considering torsion.

All reaction loads due to boundary conditions, the aerodynamic loads and the actuator loads are found using force equilibrium and compatibility equations. Then all reaction loads are combined to find the final loads working on the structure.

### 3.4 Torsion

Torsion occurs due to the actuator loads and the aerodynamic distributed loads being moved to the hinge line: the loads from actuator 1 and 2 cause torques  $M_{A1}$  and  $M_{A2}$ , respectively, while the distributed load q causes a distributed torque  $M_q$ . The magnitudes of both the load in actuator 2 and the distributed load are known, and the displacements of all three loads are known as well. Therefore, using torque equilibrium, the torque  $M_{A1}$  caused by the load in actuator 1 can be calculated, and by dividing by the arm over which it has been moved, the force itself can be found.

1 The angle of twist theta is assumed to be zero at the location of actuator 1. Calculating the angle of twist from x=0 to this point, where only the distributed torque is working, is done by rewriting the torsional stiffness equation: [2]

$$J = \frac{T}{G \frac{d\theta}{dx}} \quad (3.2)$$

Where T is the distributed torque multiplied by the distance along x, making it a function of x. This means that the angle of twist can be found with:

$$d\theta = \frac{M_q x}{GJ} dx \Rightarrow \theta = \frac{M_q}{GJ} \frac{1}{2} x^2 \quad (3.3)$$

In the section on the other side of actuator 1, this same distributed torque is acting, as well as the torques caused by the actuators. This means that in addition to the angle of twist caused by the distributed torque, these torques also contribute to the angle of twist. Thus, the following term is added to the angle of twist caused by the distributed torque as described in Equation 3.3: [2]

$$d\theta = \frac{T}{GJ} dx \Rightarrow \theta = \frac{T}{GJ} x \quad (3.4)$$

Finally, deflection caused by the torques is calculated by multiplying the angle of twist in the section under consideration by the distance of the hinge line to the leading edge and the trailing edge, to find the deflection of each of these two points.

9

## 4 Numerical model

13

In this chapter the whole process of developing a numerical model to simulate the problem at hand, as described in chapters chapter 1 and chapter 2, is outlined. Firstly section 4.1 and section 4.2 show how a conceptual model is developed to create a more workable version of the real aileron. In section 4.3, section 4.4, section 4.5 and section 4.6, the mathematical model is presented, including the governing equations, boundary conditions and initial conditions. Finally section 4.7 describes how that mathematical model is implemented into a computer program.

### 4.1 Reference frame

For the numerical model, the same frame of reference was chosen as the one shown in the assignment description. The global and local reference frame are the same. In this reference frame, the x-axis is positive pointed away from the fuselage, towards the wing tip. The z-axis is positive when pointed towards the leading edge of the wing and the y-axis is positive pointed upwards. The reference frame can be seen in Figure 4.1[4]. Sometimes, local reference frames will be used. This is shown in Figure 4.3.

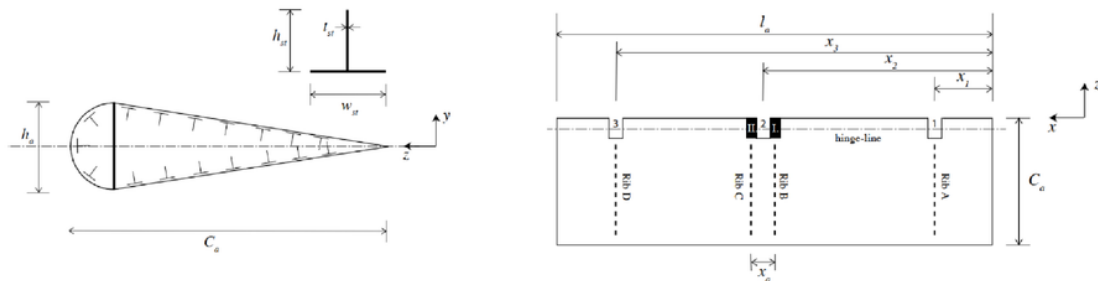


Figure 4.1: The chosen frame of reference

14

### 4.2 Structural idealization and assumptions

15

27

Compared to the overall aileron cross-section, the cross-sectional areas of the spar flanges and the stringers are small. Therefore the stress variations due to for example bending will also be relatively small. Furthermore the neutral axis is approximately equally far from the centroids of the stringers as from the centroids of the skin and these centroids are therefore assumed to coincide. For the aforementioned reasons the direct stress distribution over the stringers will be assumed constant. Subsequently the stringers and spar flanges can be replaced by concentrated areas, which are called booms. The assumption that all direct stresses are carried by the booms and all shear stresses are carried by the skin further simplifies the model and results in a skin thickness that equals zero.

In the case of the aileron cross-section, an idealization is made by replacing each of the 17 stringers by a boom. The large amount of stringers (and therefore booms) allows for the assumption that the shear flow in the skin is constant and by adding area to the booms, the direct stress carried by the skin is also accounted for. In addition, two booms are placed at the locations of the two spar flanges. This results in the geometry shown in Figure 4.2.

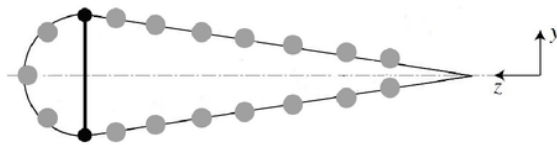


Figure 4.2: Schematic representation of the boom idealization

Further assumptions that were used for the numerical model are listed below.

- **Ribs neglected:** as the thickness of the ribs is not given but likely to be very small compared to the aileron span, the effect of this thickness on the twist and shear flow distribution over the span is assumed to be negligible. This will result in a twist that is overestimated and is therefore a conservative assumption. This assumption is also made in the analytical and validation model. 16
- **Only Steiner terms of booms counted:** in computing the area moment of inertia of the cross-section, only the Steiner terms of the booms are used, as is conventional when using structural idealization. Some trial calculations showed that most booms have a moment of inertia that is less than 1% of the value of its Steiner term about both the y- and z-axis, so, while this assumption will cause a slight underestimation in moment of inertia, the effect will be negligible. 17 In addition, it saves time. 19
- **Shear center on hinge line:** calculations showed that the shear center of the structure is located at 432.4 mm from the trailing edge, while the hinge line is located 434.5 mm from it. Due to this small difference, the shear center is assumed to lie on the chord line in all subsequent calculations.

### 4.3 Cross-sectional properties

In order to determine the deflections and stresses that the loads working on the aileron will cause on the structure, the aileron cross-section must be analysed and some of its properties must be determined, namely the centroid, the boom areas, the moment of inertia around both axes and the shear center. In these equations the reference frame shown in Figure 4.2 will be used.

Firstly, the centroid is clearly located on the chord line, due to symmetry in the z-axis. The z-coordinate of the centroid can be computed using the boom areas and locations[2]:

$$\bar{z} = \frac{\sum_1^n z_i \cdot B_i}{\sum_1^n B_i} \quad (4.1)$$

Where n is the total number of booms,  $z_i$  is the z-coordinate of a boom i, and  $B_i$  is its area. The area of a boom i is determined by taking the area of the stiffener that was originally there, and adding to it a term for each skin section adjacent to the boom. This term accounts for the thickness of the flanges and is given by[2]:

$$\frac{t_{skin}b}{6} \left( 2 + \frac{\sigma_j}{\sigma_i} \right) \quad (4.2)$$

Where b is the length of the skin panel, and  $\frac{\sigma_j}{\sigma_i}$  is the ratio between the normal stress experienced by the boom on the other end of the skin section and the boom being considered. The ratio between these normal stresses depends on the nature of the loading, hence the values of the boom area may differ as well. This ratio can be computed using distances to the neutral axis and symmetry properties. 20

For an idealized structure, the moment of inertia is calculated using only the Steiner terms of the booms. In the case of the aileron,  $I_{yz}$  is 0 due to symmetry in z. The moments of inertia about y and z are found using the following equations[2]:

$$I_{yy} = \sum_1^n (y_i - \bar{y})^2 \cdot B_i \quad (4.3)$$

$$I_{zz} = \sum_1^n (z_i - \bar{z})^2 \cdot B_i \quad (4.4)$$

The final geometrical property that should be found is the shear center, which is the point which causes no twisting of the section if an external load passes through it. Again, the y-coordinate of the shear center is known to be 0 due to symmetry in z. The z-coordinate is found by first imposing an arbitrary vertical load  $S_y$ , and finding an expression for the shear flow this load causes, which consists of the base and redundant shear flow. The base flow is calculated per skin section between each pair of adjacent booms, and is assumed to be constant in these sections. In the case of this idealized structure where only the z-coordinate of the shear center needs to be found, the base flow between two booms i and i+1 is found with the following equation:

$$q_{i+1} = -\frac{S_y}{I_{zz}}(B_i y_i) + q_i \quad (4.5)$$

By making a cut in one skin section per cell, where the base shear flow is zero, the base flows in all adjacent sections are easily calculated using above equation. Once the base flows are known, one can correct for making the cut by adding the redundant shear flow, which is a constant per cell and which can be found by imposing for each cell that:

$$\frac{d\theta}{dz} = \frac{1}{2A_{cell}} \oint \frac{q ds}{Gt} = 0 \quad (4.6)$$

Where q is the total shear flow working over the entire cell wall, i.e. the sum of all base shear flows added to the (constant) redundant shear flow. When this is written out for each cell, a system of two equations with two unknowns  $q_{s0,1}$  and  $q_{s0,2}$  is found, which can be solved. The moment caused by all shear flows is calculated around a convenient point by integrating the total shear flow per section over the section length, and multiplying this resultant force with the moment arm relative to the reference point. The z-coordinate of the shear center is then found by calculating the point at which the arbitrary shear force  $S_y$  should be applied in order to cancel out the moment caused by the shear flows.

## 4.4 Reaction forces

To determine the stresses and deflections, the reaction forces need to be calculated. This is done via a 3D setup to find all equations of motions of the combined loads. To make it easier to find all the equations of motion, some visualizations have been made with the loads and constraints given in the assignment. Loads and constraints on the aileron:

- Hinge 1 is fixed in the z-direction and displaced in the y-direction by a predefined amount.
- Hinge 2 is fixed in the x, y and z-directions.
- Hinges 3 is fixed in the z-direction and displaced in the y-direction by a predefined amount.
- Actuator I is kept fixed in the z-direction.
- Discrete load P acts in negative the z-direction at actuator II.

- Distributed load  $q$  due to aerodynamic forces on aileron, points in the negative  $y$ -direction and remains constant irrespective of any aileron deformation.
- No other than the aforementioned loads are acting on the aileron.

Figure 4.3 shows a global and local reference frame that could be used during our calculations, from which the local reference frame will be used during the project for consistency. The visualization of the load cases can be represented by Figure 4.3, Figure 4.4 and Figure 4.5. Figure 4.4 shows a local coordinate system with  $x'$ - and  $y'$ -axes. This is done to show that local reference frames is used.

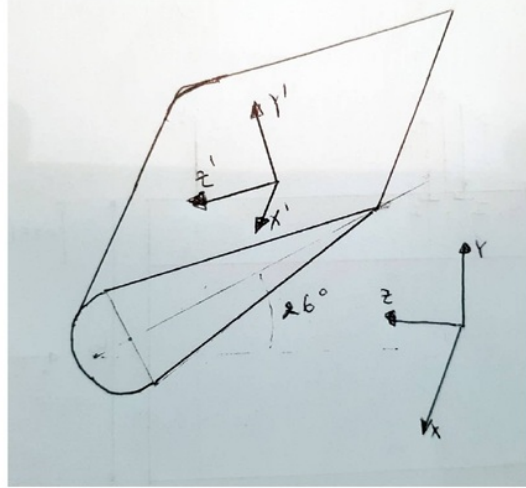


Figure 4.3: Local and Global Reference Frames

Firstly, because a local, rotated coordinate frame is used, to which the load case should be adjusted.

$$P_y = P \sin(26) \quad \text{and} \quad P_z = P \cos(26) \quad (4.7)$$

$$q_y = q \cos(26) \quad \text{and} \quad q_z = q \sin(26) \quad (4.8)$$

In order to calculate the reaction forces, the reaction forces from the actuator,  $P_{RY}$  and  $P_{RZ}$  have to be calculated first. From Figure 4.5 and Figure 4.4, Equation 4.9 can be derived.

$$\sum M_x(CCW+) = P_y \frac{h_a}{2} - P_z \frac{h_a}{2} - P_{Ry} \frac{h_a}{2} + P_{Rz} \frac{h_a}{2} - q_y(0.25c_a - \frac{h_a}{2}) = 0 \quad (4.9)$$

$M_x$  is taken around hinge 2 because the moment around the  $x$ -axis is zero over the span but for the moments around the  $y$ - and  $z$ -direction the moment is taken around  $x = 0$  because the moment is zero in this point.

Note that actually the reaction forces at hinge 1 and 3,  $R_{1z}$ ,  $R_{1y}$ ,  $R_{3z}$  and  $R_{3y}$  also create a moment around the  $x$ -axis because of the deflections  $d_{1y}$ ,  $d_{1z}$ ,  $d_{3y}$  and  $d_{3z}$  respectively. However, these moments will not be taken into account as their moment arm is relatively small and it would eventually also give more unknowns than equations. From Equation 4.9 the forces that act on actuator I,  $P_{RY}$  and  $P_{RZ}$  can be calculated.

$P_R$	93.61 [kN]
-------	------------

$$P_{RY} = P_R \sin(26) \quad (4.10)$$

$$P_{RZ} = P_R \cos(26) \quad (4.11)$$

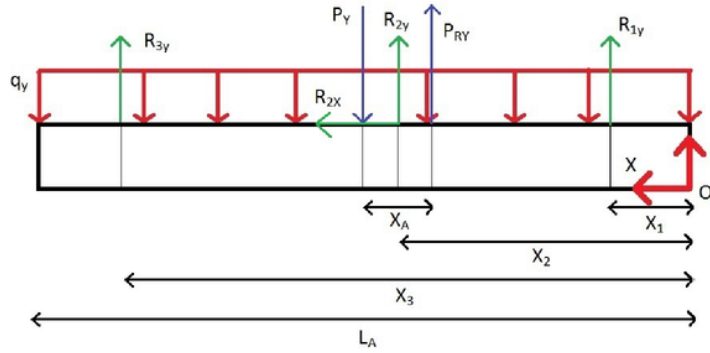


Figure 4.4: Rear view

From Figure 4.5, the following equations can be derived:

$$\sum F_x = R_{2X} = 0 \quad (4.12)$$

$$\sum F_y = R_{1y} + R_{2y} + R_{3y} + P_{Ry} - P_y - q_y \times l_a = 0 \quad (4.13)$$

$$\sum M_{z,x=0}(CW+) = R_{1y} \times x_1 + R_{2y} \times x_2 + R_{3y} \times x_3 - q_y \times \frac{l_a^2}{2} + P_{Ry} \times (x_2 - \frac{x_a}{2}) - P_y \times (x_2 + \frac{x_a}{2}) = 0 \quad (4.14)$$

The compatibility equation yields the following:

$$M_z = EI_{zz} \frac{d^2v}{dx^2} \quad (4.15)$$

Calculating the moment equation around the z-axis can be done with the use of the Macauley step function:

$$EI_{zz} \frac{d^2v}{dx^2} = q_y \frac{x^2}{2} - R_{1y} \underset{1}{\leftarrow} x - x_1 \rightarrow -P_{Ry} \underset{1}{\leftarrow} x - (x_2 - \frac{x_a}{2}) \rightarrow -R_{2y} \underset{1}{\leftarrow} x - x_2 \rightarrow +P_y \underset{1}{\leftarrow} x - (x_2 + \frac{x_a}{2}) \rightarrow -R_{3y} \underset{1}{\leftarrow} x - x_3 \rightarrow \quad (4.16)$$

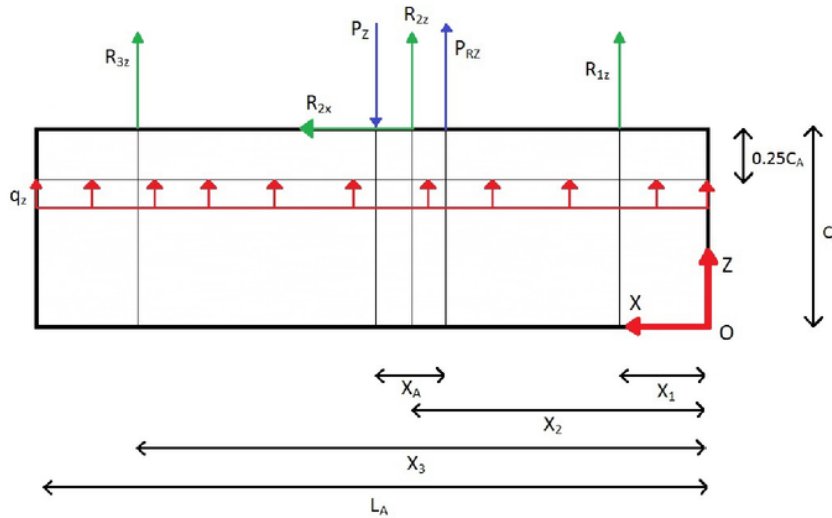
Integrate Equation 4.16 two times to end up with the compatibility equation needed to use the deflections:

$$EI_{zz}v = q_y \frac{x^4}{24} - \frac{R_{1y}}{6} \underset{1}{\leftarrow} x - x_1 \rightarrow^3 - \frac{P_{Ry}}{6} \underset{1}{\leftarrow} x - (x_2 - \frac{x_a}{2}) \rightarrow^3 - \frac{R_{2y}}{6} \underset{1}{\leftarrow} x - x_2 \rightarrow^3 + \frac{P_y}{6} \underset{1}{\leftarrow} x - (x_2 + \frac{x_a}{2}) \rightarrow^3 - \frac{R_{3y}}{6} \underset{1}{\leftarrow} x - x_3 \rightarrow^3 + c_1x + c_2 \quad (4.17)$$

Equation 4.17 will yield 3 equations for points X1, X2 and X3. These 3 equations, together with Equation 4.13 and Equation 4.14, create a system of 5 equations with 5 unknowns ( $R_{1Y}$ ,  $R_{2Y}$ ,  $R_{3Y}$ ,  $C_1$  and  $C_2$ ). The results are given in Table 4.1

$R_{1y}$	$R_{2y}$	$R_{3y}$	$C_1$	$C_2$
14.33	-24.4	20.51	10.3	-10.2

Table 4.1: Reaction forces [kN] in y-direction and integration constants



22

Figure 4.5: Top View

$$\sum F_z = R_{1Z} + R_{2Z} + R_{3Z} + P_{Rz} - P_z + q_z \times l_a = 0 \quad (4.18)$$

$$\sum M_{y,x=0}(CCW+) = -R_{1z} \times x_1 - R_{2z} \times x_2 - R_{3z} \times x_3 - q_z \times \frac{l_a^2}{2} - P_{Rz} \times (x_2 - \frac{x_a}{2}) + P_z \times (x_2 + \frac{x_a}{2}) = 0 \quad (4.19)$$

The deflections in y and z at all three hinges are used as boundary conditions to make up our compatibility equations. Just like Equation 4.17, the compatibility equation for the moment around the y-axis can be created and looks as follows:

$$EI_{yy} \frac{d^2v}{dx^2} = q_z \frac{x^2}{2} + \boxed{R_{1z} < x - x_1 >} + P_{Rz} < x - (x_2 - \frac{x_a}{2}) > + \boxed{R_{2z} < x - x_2 >} \\ - \boxed{P_z < x - (x_2 + \frac{x_a}{2}) >} + \boxed{R_{3z} < x - x_3 >} \quad (4.20)$$

Integrate Equation 4.20 two times to end up with the compatibility equation needed to use the deflections.

$$EI_{yy}v = q_z \frac{x^4}{24} + \frac{R_{1z}}{6} < x - x_1 >^3 + \frac{P_{Rz}}{6} < x - (x_2 - \frac{x_a}{2}) >^3 + \frac{R_{2z}}{6} < x - x_2 >^3 \\ - \frac{P_z}{6} < x - (x_2 + \frac{x_a}{2}) >^3 + \frac{R_{3z}}{6} < x - x_3 >^3 + D_1x + D_2 \quad (4.21)$$

The deflections at points X1, X2 and X3, which are  $\delta_{1Z}$ , 0 and  $\delta_{3Z}$  respectively. In total 5 equations are obtained with 5 unknowns ( $R_{1Z}$ ,  $R_{2Z}$ ,  $R_{3Z}$ ,  $D_1$  and  $D_2$ ). The results are given in Table 4.2.

$R_{1z}$	$R_{2z}$	$R_{3z}$	$D_1$	$D_2$
-50.25	67.27	-24.24	26.72	-22.47

Table 4.2: Reaction forces [kN] in z-direction and integration constants

## 4.5 Torsion

The torsion  $T$  was calculated in the following way, using Figure 4.6.

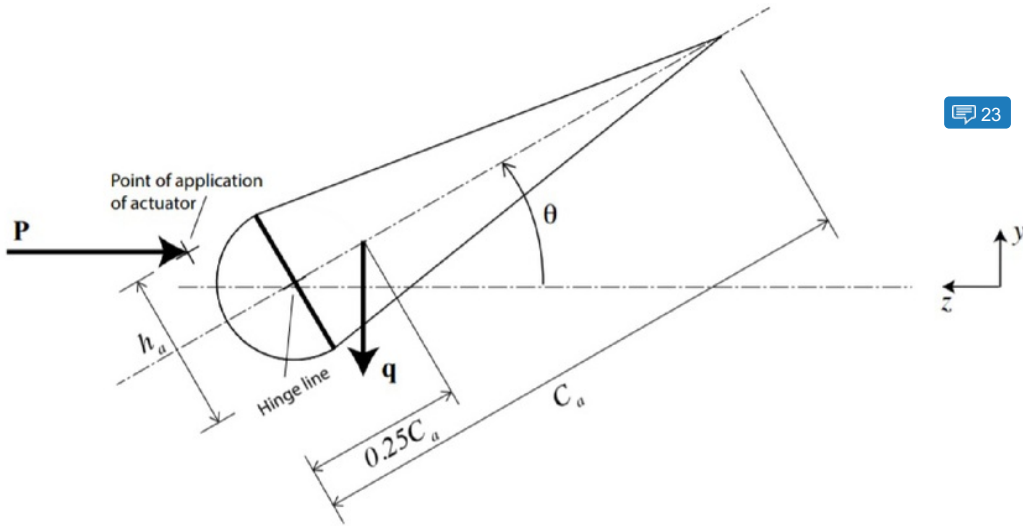


Figure 4.6: Torque Calculation

Assuming the depicted point of application and distances in Figure 4.6 the following formulae for the torque can be derived:

For  $0 < X < X_2 - \frac{X_A}{2}$ :

$$T = -q_Y X (0.25C_A - (C_A - X_{SC})) \quad (4.22)$$

For  $X_2 - \frac{X_A}{2} < X < X_2 + \frac{X_A}{2}$ :

$$T = -q_Y X (0.25C_A - (C_A - X_{SC})) - P_{RY}(C_A - X_{SC}) + P_{RZ} \frac{H_A}{2} \quad (4.23)$$

For  $X_2 + \frac{X_A}{2} < X < L_A$ :

$$T = -q_Y X (0.25C_A - (C_A - 0.4324)) - P_{RY}(C_A - X_{SC}) + P_{RZ} \frac{H_A}{2} + P_Y(C_A - X_{SC}) - P_Z \frac{H_A}{2} \quad (4.24)$$

With  $X_{SC}$  equal to the x-location of the shear center, which is at 0.4324 m seen from the Trailing edge of the aileron.

## 4.6 Shear flows and Deflection

The torsion and shear loads that act on the aileron cause a shear flow in its structure and will cause the structure to twist around the x-axis. Furthermore the bending loads on the aileron cause the aileron to deflect in y-direction. Find the effects of torsion in subsection 4.6.1, the effects of shear in subsection 4.6.2 and the deflection due to bending in subsection 4.6.3.

### 4.6.1 Due to Torsion

As the loads on the aileron do not act in the shear center, they will produce a torque around the x-axis. In the analysis of the shear flows and twist, the loads are considered to act in the shear center with an additional torque applied. Since purely torque is considered in this section, the booms play no part in the analysis. The shear flow is assumed to act as shown in Figure 4.7.

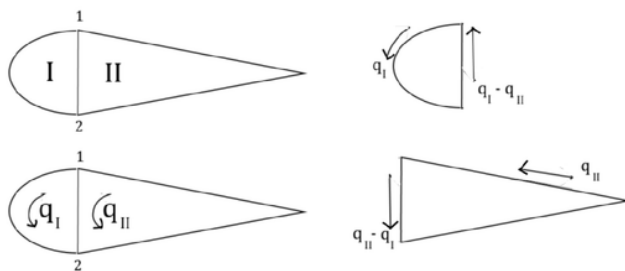


Figure 4.7: Schematic representation of the assumed shear flow

To solve for the three unknowns  $q_{soI}$ ,  $q_{soII}$  and  $\frac{d\theta}{dz}$ , three equations are needed, as specified below in Equation 4.25 and Equation 4.26 for the rate of twist as a function of x and Equation 4.27 for the total torque in the section [3]. The distortion between the two cells is likely negligible and therefore the rate of twist in the two cells is assumed to be equal.

$$\left( \frac{d\theta}{dx} \right)_I = \frac{1}{2A_I G} \left( \frac{q_1 \Delta s_{skin1-2}}{t_{skin}} + \frac{(q_I - q_{II}) \Delta s_{spar2-1}}{t_{spar}} \right) \quad (4.25)$$

$$\left( \frac{d\theta}{dx} \right)_{II} = \left( \frac{d\theta}{dx} \right)_I = \frac{1}{2A_{II} G} \left( \frac{(q_{II} - q_1) \Delta s_{spar1-2}}{t_{spar}} + \frac{q_{II} \Delta s_{skin2-1}}{t_{skin}} \right) \quad (4.26)$$

$$T = 2A_I q_I + 2A_{II} q_{II} \quad (4.27)$$

### 4.6.2 Due to Shear

As the two cell wing box is a statically indeterminate structure, a cut is made in each cell to make the structure statically determinate. The 'open section' shear flow, or base shear flow  $q_b$  as it will be called from now on is calculated, to which the redundant shear flow  $q_{so}$  for each cell is added. The redundant shear flow in the top skin panel is usually small and this is where the cuts are positioned to avoid numerical errors coming from the large difference in significant digits in the base and redundant shear flow. First, the base shear flow is calculated using Equation 4.28 for an idealized structure with zero second moment of area (see [2] for the derivation of Equation 4.28, Equation 4.29).

$$q_b = -\frac{V_x}{I_{yy}} \sum_{r=1}^n B_r x_r - \frac{V_y}{I_{xx}} \sum_{r=1}^n B_r y_r \quad (4.28)$$

Using the values for the base shear flow between each boom, the rates of twist can be calculated for each cell, which are again assumed to be equal, as in subsection 4.6.1.

For the  $i$ th cell:

$$\frac{d\theta}{dx_i} = \frac{1}{2A_i} \oint \frac{(q_{bi} + q_{s0i})ds}{t_i G_i} \quad (4.29)$$

To verify the values for the open section shear flow  $q_b$ , vertical and horizontal equilibrium can be checked.

$$V_z = q_{bz} * L \quad (4.30)$$

One more equation is then needed to solve for the three unknowns  $q_{s0I}$ ,  $q_{s0II}$  and  $\frac{d\theta}{dz}$ . The moment around an arbitrary point O, caused by the shear forces on the structure, must equal the moment of the shear flow around that point. The moment  $M_o$  caused by the shear loading with arm p is

$$M_o = \sum_{i=1}^N q_{bi} p_i ds + \sum_{i=1}^N q_{s0i} \oint p_i ds \quad (4.31)$$

To ease the calculations, point O is chosen where the symmetry axis coincides with the spar. In this way, the moment is approximately equal to the torque in the section and the integrals as a function of arm  $p$  are simpler.

#### 4.6.3 Due to Bending

Now that the reaction forces are known, the bending moment created by the shear forces in other sections of the wing can be calculated and be equated to the deflection of the hinge line. The bending moment causes a direct stress in the structure, which is carried completely by the booms in the idealized structure (the booms account for the skin as well). The direct stresses in the booms are found from Equation 4.32, which takes into account that the second moment of area  $I_{zy}$  is zero [2].

$$\sigma_x = \frac{M_z}{I_{zz}} y + \frac{M_y}{I_{yy}} x \quad (4.32)$$

The relationship with  $v$  being the deflection of the hinge is:

$$\begin{aligned} EI_{yy}v &= q_z \frac{x^4}{24} + \frac{R_{1z}}{6} < x - x_1 >^3 + \\ \frac{P_{Rz}}{6} &< x - (x_2 - \frac{x_a}{2}) >^3 + \frac{R_{2z}}{6} < x - x_2 >^3 \\ -\frac{P_z}{6} &< x - (x_2 + \frac{x_a}{2}) >^3 + \frac{R_{3z}}{6} < x - x_3 >^3 + c_1 x + c_2 \end{aligned}$$

 24

#### 4.7 Computational model

In this section the implementation of the mathematical program into the computer program is explained. The separate identifiable code blocks and their interrelation, as well as their individual inputs and outputs can be  read from flowchart Figure 4.8. Furthermore, the workings of the code are described using pseudocode in subsection 4.7.1 and subsection 4.7.2 respectively.  25

In the computational model, the aileron has been discretized into 113 sections along the span. A test using 100 times as many sections showed that the effect was less than 0.1%, but took more computational time.

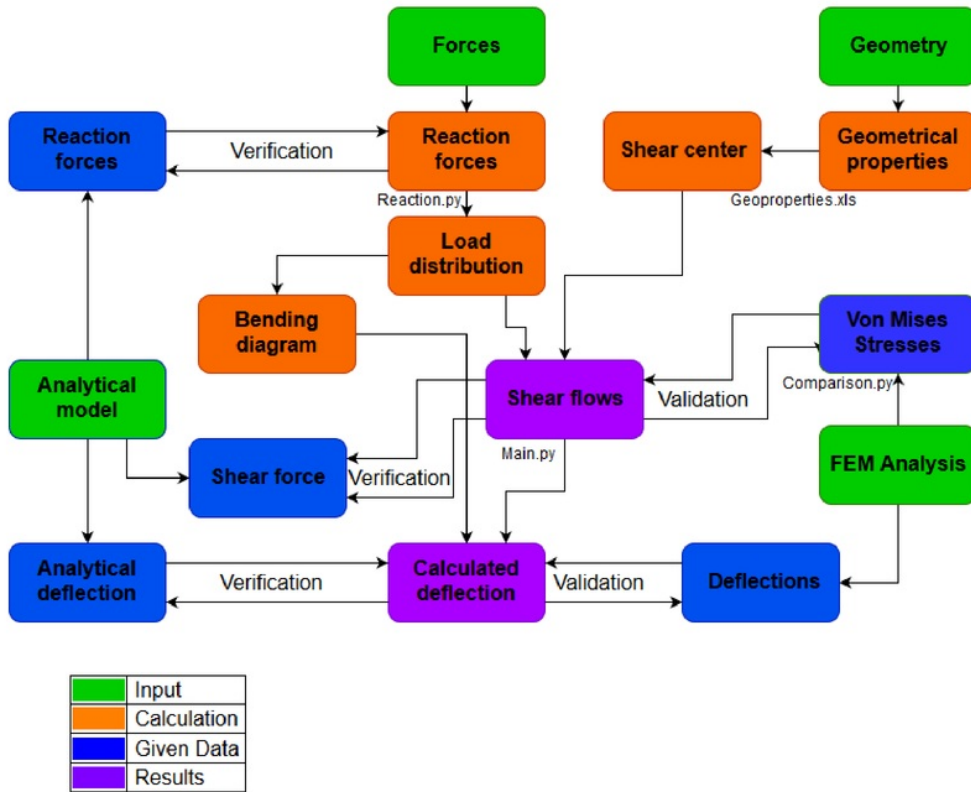


Figure 4.8: Flowchart

#### 4.7.1 Reaction forces code

26

```
#Import modules
import numpy, math
import matplotlib

#Definitions
define distances
define geometric properties
define loads

#Find reaction force actuator
Pr = take moments around x-axis

#Reaction forces in y direction and integration constants
#5 equations, 5 unknowns

eq1, eq2, eq3, eq4, eq5 = Moments around y, sum of forces y-direction, deflection equation
a = equations left side
b = equations right side

y = solve(a,b)
```

```
#Reaction forces in z direction and integration constants
#5 equations, 5 unknowns

eq1, eq2, eq3, eq4, eq5 = Moments around z, sum of forces z-direction, deflection equation
a = equations left side
b = equations right side

z = solve(a,b)

#Check
Add forces

#Load diagrams
Make free body diagram
Put all values in list

for i in range(sections):
    assign a value to each section
    shearlist.append(value)
    multiply value to its x-distance
    momentlist.append(value)
    multiply value to its z-value
    torsionlist.append(value)

#Plotting
Plot shear, moment, torsion diagram
```

#### 4.7.2 Shear flows and twist code

```
#Import modules
import numpy
import matplotlib
import reactions.py
import pandas #For validation

#Definitions
define sections
define geometric properties

#Calculations
Calculate constants and distances

#Torsion
Make empty arrays
for i in range(sections):
    #3 equations, 3 unknowns
    eq1, eq2, eq3 = 2 deflection equation, 1 Torque equation (around shear center)
    a = equations left side
    b = equations right side
    x = solve(a,b)
```

```

#Open section shear flows
for i in range(sections):
    for j in range(20):
        Calculate base shear flow

#Twist and closed section shear flow
for i in range(sections):
    #3equations, 3 unknowns
    eq1, eq2, eq3 = 2 deflection equation, 1 moment equation (around centroid)
    a = equations left side
    b = equations right side
    x = solve(a,b)
    add base shear flow with closed section shear flow

#Total deflection LE and TE
for i in range (sections):
    LEdeflection = -twist*xdistance*ydistance
    TEdeflection = twist*xdistance*ydistance

#Von Mises stresses
for i in range(sections):
    for j in range(20):
        VMstresses = shear/length + bending*ydistance/ZInertia

#Validation data
for i in range(sections):
    Vali_stress[i] = dataset["MiseStress"]
    if dataset["MiseStress"] == 0.0 :
        Vali_stress[i] = Vali_stress[i-1]

#Plotting
plot

```

## 5 Verification

 27

After the completion of the numerical model, this model was verified using an analytical model, provided by the course instructors. The verification is a vital part of proving that the program works and produces accurate results. The results of this verification are described in this chapter.

### 5.1 Code verification and Calculation Verification

 28

During the writing of the code, the code was also verified. Errors were filtered out. The program gave a lot of wrong answers in first instance. To check where the mistake occurred, a print statement was put before every step in the calculations and in this way each unit was checked before proceeding to the next unit of code. In this way, a lot of results were displayed and the step where a false outcome was found, could be adjusted. If then the outcome was still wrong, the calculations themselves had to be verified.

## 5.2 Comparison

This section will describe how the numerical model compares to the analytical model. The geometrical properties are compared in subsection 5.2.1 and the reaction forces are compared in subsection 5.2.2. The result of these forces; shear moment and torsion are compared to the analytical model in subsection 5.2.3 and subsection 5.2.4 respectively.

### 5.2.1 Geometrical properties

As explained in chapter 3, in the analytical model it seems that the centroid was initially assumed to be located on the hinge line. Due to the fact that this resulted in a very large deviation from the centroid location calculated in the numerical model, a more accurate calculation was made to find a centroid to be used for subsequent calculations. This new centroid was found to be located at  $z=317.9$  mm, versus a value of  $z=304.9$  mm found in the numerical model. This is a difference of  $\frac{317.9-304.9}{317.9} * 100\% = 4.1\%$  and thus seems reasonable. As for the moments of inertia of the cross-section:

$$\frac{I_{yy,\text{analytical}} - I_{yy,\text{numerical}}}{I_{yy,\text{analytical}}} * 100\% = \frac{6.20 * 10^7 - 5.20 * 10^7}{6.20 * 10^7} * 100\% = 16.2\% \quad (5.1)$$

29

$$\frac{I_{zz,\text{analytical}} - I_{zz,\text{numerical}}}{I_{zz,\text{analytical}}} * 100\% = \frac{1.25 * 10^7 - 1.20 * 10^7}{1.25 * 10^7} * 100\% = 4.18\% \quad (5.2)$$

1 Clearly, there is a difference between the moment of inertia obtained through the numerical and the analytical model, especially in the moment of inertia about the y-axis. These differences can be explained by considering the differences in methods used: by choosing to only count the boom Steiner terms in the numerical model, the moments of inertia of each component about its own centroid is neglected. In the case of the aileron, the lower and upper skin in the section to the right of the spar have a very large contribution to the area moment of inertia about y: at  $7767314\text{mm}^4$  each, these are the main causes of the large difference. Smaller differences in moment of inertia about both the y- and z- axis are due to difference in component spacing with respect to the structural idealization geometry.

### 5.2.2 Reaction forces

Comparing the reaction forces, calculated in the numerical model, with the ones from the analytical model some differences were found and will be explained here.

	Numerical model [kN]	Analytical model [kN]	Difference [kN]	Difference [%]
R1y	14.33	18.67	-4.34	30.1
R1z	-50.25	-58.26	8.01	15.94
R2y	-24.4	-32.61	8.21	33.64
R2z	67.27	80.95	-13.68	20.0
R3y	20.51	24.04	-3.53	17.2
R3z	-24.24	-30.62	6.38	26.3
Pr	93.61	94.41	-0.8	0.85

30

Table 5.1: Comparison reaction forces

First of all the combined reaction forces were compared and it is concluded that there is quite a big difference with the analytical model, looking at Table 5.1. the maximum difference that is found is 33.64 percent. The first thought was that some minor mistakes were made in the inputs, calculations or the set up of the equations but no such mistakes were found. In subsection 5.2.1 it is stated that the moments of inertia both have a difference so to check if the calculations are correct, the moment of inertia of the analytical model is used in the numerical model. By doing this, the result showed that the reaction forces in z-direction are almost identical but that reaction force in y-direction still have a maximum difference of 25 percent. After this comparison, only the reaction forces calculated with the boundary conditions were compared with the ones in the analytical model. Now it was seen that all reaction forces were identical. Therefore it can be stated that our inputs and calculations are correct. The reason why the reaction forces in y-direction still have such a big difference is because of the assumption in the analytical model that  $q$ ,  $P$  and  $P_R$  do not contribute to the deflection when calculating the reaction forces. The relatively low  $I_{zz}$  means that contribution of the  $q$ ,  $P$  and  $P_R$  is significant and cannot be neglected. Hence, the numerical solution is therefore more accurate than the analytical model. Although showing the same behaviour, a larger discrepancy of up to 25 percent with the analytical model can still be found. The reason for this difference is thus that the assumption that all forces contribute to the deflection was used. It has also been checked if the differences between the reaction forces in the numerical and analytical model are the same when the angle  $\theta$  is changed. The differences between the reaction forces for  $\theta$  equal to 0 and 26 are different from each other and should normally be the same. The reason for this can be due to the differences in moment of inertia. As well the method that is used in the numerical and analytical model because when the angle is changed to 0 degrees, the distributed load only acts in the z-direction and the point load only acts in the y-direction. Therefore a change will be found between the difference of the percentages between the numerical and analytical model when the angle is changed from 26 to 0 degrees.

31

1 While looking at the reaction forces in the analytical model it was seen that the reaction forces for the global reference frame where calculated in the wrong way. The reason for this is that a wrong input was used and sign had to be changed. Therefore if the global reference system was used to calculate the reaction forces, some problems will have occurred because of these mistakes.

### 5.2.3 Shear and Moment Diagrams

Because of these differences in reaction forces, the shear and moment graphs from the analytical model were compared with the graphs from the numerical model. From this, it was observed that the shear diagrams were almost exactly the same with relatively small differences at each point, but that one of the moment diagrams was different. Firstly the analytical model used the data corresponding to the moment around the y-axis for the  $M_z$ -diagram and the data corresponding to the moment around the z-axis for the  $M_y$ -diagram, so it was basically turned around.

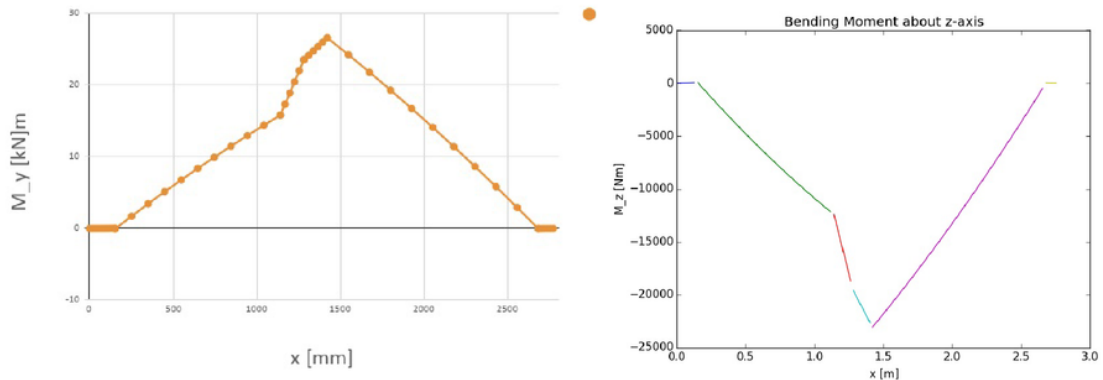


Figure 5.1: Comparison of bending moments about Z for analytical (left) and Numerical (right) model

When looking at the graphs, it can be observed that they have the same form, but that firstly they have different values. This is because in first instance, the reaction forces did not perfectly correspond to each other and the moment diagram uses the reaction force values as its input. Secondly they are each others mirror images about the x-axis. This is due to the fact that the numerical model used the coordinate system showed in Figure 4.4 with the clockwise direction defined as the positive direction, which eventually yields negative moment slopes for positive corresponding shear forces, which does not sound quite right. The analytical model took the shear forces diagram and integrated this once. This resulted in positive moment diagram slopes for positive corresponding shear forces. Eventually, this is how the numerical model should have done it as well. The correction that can be made for this is to multiply the moment diagram by -1 to obtain the right form as shown in the left part of Figure 5.2.

32

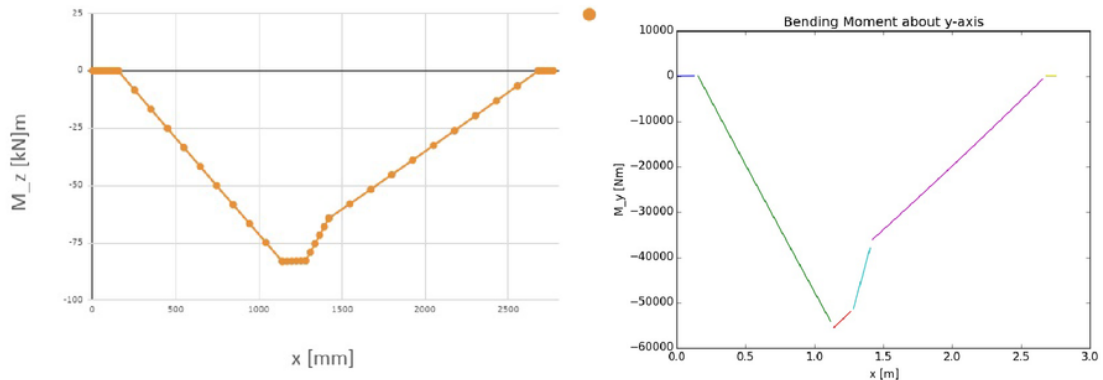


Figure 5.2: Comparison of bending moments about Y for analytical (left) and Numerical (right) model

From the Figure 5.2 it can clearly be seen that the graphs have the same form, but that their values differ by a pretty big amount. This is because the reaction forces from the numerical model and the analytical model do not entirely match. This affects the shear and moment diagrams.

### 5.2.4 Torsion Diagram

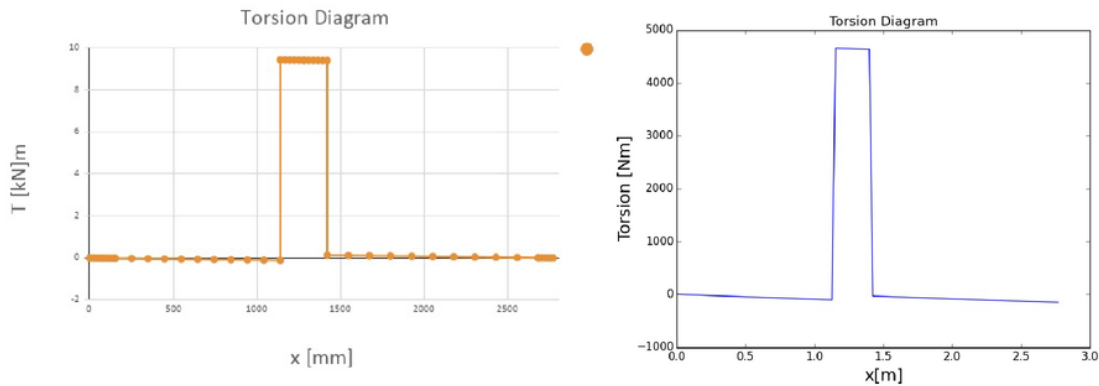


Figure 5.3: Comparison of torsion diagrams for analytical (left) and Numerical (right) model

What can be deducted from Figure 5.3 is that the forms of the 2 graphs have pretty much the same form, but that the values differ. This is because the formulae for the torsion from the analytical model are different from the formulae for the torsion from the numerical model, which can be found in section 4.5.

33

34

# 6 Validation

35

The data that was given for validation came from a finite element method (FEM) analysis. In reality the data should come from a real part test, but since a hypothetical case is analyzed, the only available results can come from a FEM solution. This means that the data comes in .odb files. In order to validate the data that the numerical model produces, there should be a comparison between the model and the FEM data. However, the data that was given is not in the same format. First, the assumptions needed for the validation are listed. Secondly, the transformation of the data that is needed for comparison is explained. Finally, the results of the validation are discussed including the corrections that it requires.

## 6.1 Assumptions

- Von Mises stresses only consists because of shearflow and bending
- The Von Mises stresses on each section is the average of the upper and lower stress in the segment
- The average stresses of the FEM segments that correspond to a model segment is representative.
- The average deflection of the FEM segments that correspond to a model segment is representative.
- The ribs are neglected

## 6.2 Experimental Data Description

The Experimental Data were found in .zip files on the Brightspace page of course AE3212-II, which contained the results of a FEM analysis of the airfoil. The results consisted of .rpt files that could be opened with excel. These files provided x/y/z coordinates and the infamous Von Mises stresses of every section. The results of the numerical model however were not Von Mises stresses. They needed to be transformed using the following equations:

$$\sigma_{VonMises} = \sqrt{\sigma_u^2 + 3\tau_{vw}^2} \quad (6.1)$$

36

$$\sigma_u = \frac{M_w v}{I_{ww}} \quad (6.2)$$

$$\tau_{vw} = \frac{q_{vw}}{t} \quad (6.3)$$

## 6.3 Data transformation

18

The provided stresses data was given in x/y/z coordinates in the local coordinate system. The files also contained many more data points than the numerical model would provide. Whilst the data from the numerical model was divided in 20 sections around the skin and 113 sections over the span. To be able to compare the data points, the coordinates have to be adjusted as the following:

First the upper and lower sides of the nodal stresses were averaged so that the skin could be divided into 20 sections. Secondly the nodes were linked to the coordinate system so that it would be possible to order them. Finally the nodes were reordered to have the same order of discretization. This means starting at  $x = 0$  and the trailing edge moved over the lower side to the leading edge and over the upper skin back. Then move one discretization towards the tip of the aileron.

## 6.4 Comparison

Combining the stresses from shear, torsion and bending. The Von Mises stresses of the numerical model were obtained. Looking at the graph the values seem reasonable. However the two lines did not match by far. One of the reasons for this was that most of the data from the validation model were zero or very small. This is due to the fact that data was unreadable when it was transformed to excel and read by python. This rendered the data quite useless and proved the task of corrected the numerical model impossible. Nonetheless Figure 6.1 is presented to show the differences between the model and the FEM analysis.

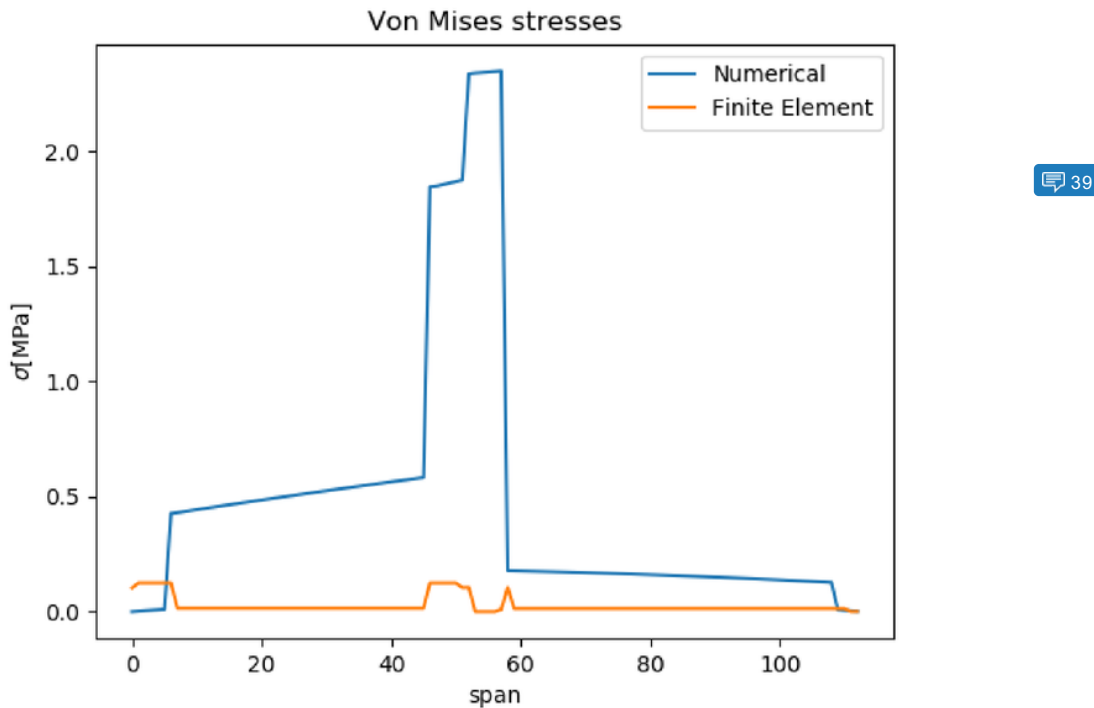


Figure 6.1: Von Mises stresses

## 7 Conclusion

The aileron is a crucial component of the aircraft's wing. For this reason it is very important to know how it will behave under certain load cases. This report shows the calculations that are made to obtain the maximum deflections and shear flow during the most critical condition that the aileron has to endure. These calculations inevitably contain errors in the first place and have been verified using a simplified model that has been solved analytically.

The problem has been analyzed in the local coordinate frame and solved with the help of a boom idealization. 19 booms scattered around the rib and the span were divided in 113 sections. The geometrical properties and reaction forces have been determined with same approach that has been introduced in the AE2180-II Structural analysis course [3]. The shear flows have been calculated using equations from the book [2]. The report also gives a detailed description of the code that have been used for the calculations in the form of a pseudocode.

After the results were obtained from the analytical and numerical model, these were compared to analyze and correct for the differences. After the corrections in the analytical model, the geometrical properties only had few differences, these can be explained by the differences in approach and assumptions. The reaction forces however had many more differences. This was due to some of the mistakes made in the analytical model.

When the numerical model was completely verified with the analytical model, it was compared to the results of the FEM analysis. This proved rather useless when most of the data points disappeared during the transformation from .rpt files to the python program. In conclusion, the problem statement has been answered up to the extent that the validation has not been done successfully, but from verification the results seemed valid.

# Bibliography

- [1] <HTTP://ASM.MATWEB.COM/SEARCH/SPECIFICMATERIAL.ASP?BASSNUM=MA2024T3>. Aluminim 2024-t3 asm material data sheet.
- [2] MEGSON, T. *Aircraft structures for Engineering Students*, fifth ed. Elviesier aerospace engineering series. Elsevier Ltd., 2007.
- [3] VAN CAMPEN, J. *Slides introduction lecture*. 2019.
- [4] VAN DER WAL, W. *SVV Structures assignment*. 2019.

# Work Distribution

Tasks	Intro	Problem analysis	Analytical model	Numerical model	Verification	Validation	Conclusion
Nick	4,0	0,0	1,0	28,0	2,0	15,0	2,0
Angela	2,0	3,0	8,0	22,0	10,0	0,0	0,0
Reinier	0,0	0,0	0,0	20,0	1,0	32,0	0,0
Andreas	0,0	0,0	0,0	33,0	20,0	0,0	0,0
Luc	0,0	5,0	0,0	27,0	10,0	0,0	1,0
Willem	0,0	2,0	2,0	40,0	5,0	5,0	1,0

# Code Loads

```

12
import numpy as np
from math import *
import matplotlib.pyplot as plt

# given properties
La = 2.771 # m
ca = 0.547 # m
D1 = 110.3 # m
d1y = D1 * cos(radians(26))
d1z = D1 * sin(radians(26))
D3 = 164.2 # m
d3y = D3 * cos(radians(26))
d3z = D3 * sin(radians(26))

E = 73.1e9 # Pa
Izz = 1.252e-5
Iyy = 6.203e-5
x1 = 0.153 # m
x2 = 1.281 # m
x3 = 2.681 # m
xa = 0.28 # m
Ha = 0.225 # m

P = 91.7 * 1000 # N
py = P * sin(radians(26)) # N
pz = P * cos(radians(26)) # N
q = 4.53 * 1000 # N/m
qy = q * cos(radians(26)) # N
qz = q * sin(radians(26)) # N

# Moment around x-axis find reaction force actuator

#  $O = -qy*(0.25*ca-Ha/2)-pz*Ha/2+py*Ha/2+Pr*(cos(radians(26))*Ha/2-sin(radians(26))*Ha/2)$ 
1
Pr = (qy * (0.25 * ca - Ha / 2) + pz * Ha / 2 - py * Ha / 2) / (cos(radians(26)))
* Ha / 2 - sin(radians(26)) * Ha / 2)
pry = Pr * sin(radians(26))
prz = Pr * cos(radians(26))

# Reaction forces in y-direction and integration constants
# 5 functions 5 unknowns -> Moments around z-direction, sum of forces in y-direction
# and deflection function

a = np.array(1
[[0, 0, 0, x1, 1], [-(x2 - x1) ** 3 / 6, 0, 0, x2, 1], [-(x3 - x1) ** 3 / 6,

```

```


$$-(x_3 - x_2)^{3/6}, 0, x_3, 1], [1, 1, 1, 0, 0], [x_1, x_2, x_3, 0, 0])$$

b = np.array([-E * Izz * diy - qy * x1 ** 4 / 24,
              pry * (xa / 2) ** 3 / 6 - qy * x2 ** 4 / 24,
              -E * Izz * d3y - py * (x3 - x2 - xa / 2) ** 3 / 6 - qy * x3 ** 4 / 24
              + pry * (x3 - x2 + xa / 2) ** 3 / 6,
              qy * La + py - pry,
              qy * La ** 2 / 2 + py * (x2 + xa / 2) - pry * (x2 - xa / 2)])
```

y = np.linalg.solve(a, b)

R1y = y[0]  
R2y = y[1]  
R3y = y[2]  
c1 = y[3]  
c2 = y[4]

# Reaction forces in z-direction and integration constants

```

c = np.array([[0, 0, 0, x1, 1], [(x2 - x1) ** 3 / 6, 0, 0, x2, 1], [(x3 - x1) ** 3 / 6,
              (x3 - x2) ** 3 / 6, 0, x3, 1], [1, 1, 1, 0, 0], [x1, x2, x3, 0, 0]])
```

d = np.array([-E \* Iyy \* d1z - qz \* x1 \*\* 4 / 24,
 -qz \* x2 \*\* 4 / 24 - prz \* (xa / 2) \*\* 3 / 6,
 -qz \* x3 \*\* 4 / 24 + pz \* (x3 - x2 - xa / 2) \*\* 3 / 6 -
 prz \* (x3 - x2 + xa / 2) \*\* 3 / 6 - E \* Iyy \* d3z,
 -prz + pz - qz \* La,
 -qz \* La \*\* 2 / 2 + pz \* (x2 + xa / 2) - prz \* (x2 - xa / 2)])

z = np.linalg.solve(c, d)

R1z = z[0]  
R2z = z[1]  
R3z = z[2]  
e1 = z[3]  
e2 = z[4]

# check

t1 = R1y + R2y + R3y + pry - py - qy \* La  
t2 = R1z + R2z + R3z + prz - pz + qz \* La

# Ranges

```

section = 1000
s1 = np.arange(0, x1, 0.0255)
s2 = np.arange(x1, x2 - xa / 2, 0.0247)
s3 = np.arange(x2 - xa / 2, x2, 0.024522)
s4 = np.arange(x2, x2 + xa / 2, 0.024522)
s5 = np.arange(x2 + xa / 2, x3, 0.024706)
s6 = np.arange(x3, La, 0.024522)
```

```
def lijst(x):
    m = []
    for i in x:
        m.append(i)

    return m

# Moment diagram x-y plane

my1 = qy / 2 * s1 ** 2
my2 = qy / 2 * (s2) ** 2 - R1y * (s2 - x1)
my3 = qy / 2 * (s3) ** 2 - R1y * (s3 - x1) - pry * (s3 - (x2 - xa / 2))
my4 = qy / 2 * (s4) ** 2 - R1y * (s4 - x1) - pry * (s4 - (x2 - xa / 2))
    - R2y * (s4 - x2)
my5 = qy / 2 * (s5) ** 2 - R1y * (s5 - x1) - pry * (s5 - (x2 - xa / 2))
    - R2y * (s5 - x2) + py * (s5 - (x2 + xa / 2))
my6 = qy / 2 * (s6) ** 2 - R1y * (s6 - x1) - pry * (s6 - (x2 - xa / 2))
    - R2y * (s6 - x2) + py * (s6 - (x2 + xa / 2)) - R3y * (s6 - x3)

m1 = lijst(my1)
m2 = lijst(my2)
m3 = lijst(my3)
m4 = lijst(my4)
m5 = lijst(my5)
m6 = lijst(my6)

# missing 0.00134m in span parts

MZ = m1 + m2 + m3 + m4 + m5 + m6

# Shear diagram x-y plane

vy1 = -qy * s1
vy2 = -qy * s2 + R1y
vy3 = -qy * s3 + R1y + pry
vy4 = -qy * s4 + R1y + pry + R2y
vy5 = -qy * s5 + R1y + pry + R2y - py
vy6 = -qy * s6 + R1y + pry + R2y - py + R3y

v11 = lijst(vy1)
v22 = lijst(vy2)
v33 = lijst(vy3)
v44 = lijst(vy4)
v55 = lijst(vy5)
v66 = lijst(vy6)

VY = v11 + v22 + v33 + v44 + v55 + v66

# Moment diagram x-z plane
```

```

mz1 = qz / 2 * s1 ** 2
mz2 = qz / 2 * (s2) ** 2 + R1z * (s2 - x1)
mz3 = qz / 2 * (s3) ** 2 + R1z * (s3 - x1) + prz * (s3 - (x2 - xa / 2))
mz4 = qz / 2 * (s4) ** 2 + R1z * (s4 - x1) + prz * (s4 - (x2 - xa / 2))
+ R2z * (s4 - x2)
mz5 = qz / 2 * (s5) ** 2 + R1z * (s5 - x1) + prz * (s5 - (x2 - xa / 2))
+ R2z * (s5 - x2) - pz * (s5 - (x2 + xa / 2))
mz6 = qz / 2 * (s6) ** 2 + R1z * (s6 - x1) + prz * (s6 - (x2 - xa / 2))
+ R2z * (s6 - x2) - pz * (s6 - (x2 + xa / 2)) + R3z * (s6 - x3)

m11 = lijst(mz1)
m22 = lijst(mz2)
m33 = lijst(mz3)
m44 = lijst(mz4)
m55 = lijst(mz5)
m66 = lijst(mz6)

MY = m11 + m22 + m33 + m44 + m55 + m66

# Shear diagram x-z plane

vz1 = qz * s1
vz2 = qz * s2 + R1z
vz3 = qz * s3 + R1z + prz
vz4 = qz * s4 + R1z + prz + R2z
vz5 = qz * s5 + R1z + prz + R2z - pz
vz6 = qz * s6 + R1z + prz + R2z - pz + R3z

v1 = lijst(vz1)
v2 = lijst(vz2)
v3 = lijst(vz3)
v4 = lijst(vz4)
v5 = lijst(vz5)
v6 = lijst(vz6)

VZ = v1 + v2 + v3 + v4 + v5 + v6

# torsion diagram (moment around shear center with x_ (shear center) = ca - 0.4324 m  
as seen from the leading edge)

t1 = -qy * s1 * (0.25 * ca - (ca - 0.4324))
t2 = -qy * s2 * (0.25 * ca - (ca - 0.4324))
t3 = -qy * s3 * (0.25 * ca - (ca - 0.4324)) - pry * (ca - 0.4324)
+ prz * Ha / 2
t4 = -qy * s4 * (0.25 * ca - (ca - 0.4324)) - pry * (ca - 0.4324)
+ prz * Ha / 2
t5 = -qy * s5 * (0.25 * ca - (ca - 0.4324)) - pry * (ca - 0.4324)
+ prz * Ha / 2 + py * (ca - 0.4324) - pz * Ha / 2
t6 = -qy * s6 * (0.25 * ca - (ca - 0.4324)) - pry * (ca - 0.4324)

```

```

+ prz * Ha / 2 + py * (ca - 0.4324) - pz * Ha / 2

t11 = lijst(t1)
t22 = lijst(t2)
t33 = lijst(t3)
t44 = lijst(t4)
t55 = lijst(t5)
t66 = lijst(t6)

# list with torsion for predefined x-values
T = t11 + t22 + t33 + t44 + t55 + t66

# plotting diagrams

# moment x-y plane
plt.subplot(5, 1, 1)
plt.title('my')
plt.plot(s1, my1, s2, my2, s3, my3, s4, my4, s5, my5, s6, my6)

# shear x-y plane
plt.subplot(5, 1, 2)
plt.title('vy')
plt.plot(s1, vy1, s2, vy2, s3, vy3, s4, vy4, s5, vy5, s6, vy6)

# moment x-z plane
plt.subplot(5, 1, 3)
plt.title('mz')
plt.plot(s1, mz1, s2, mz2, s3, mz3, s4, mz4, s5, mz5, s6, mz6)

# shear x-z plane
plt.subplot(5, 1, 4)
plt.title('vz')
plt.plot(s1, vz1, s2, vz2, s3, vz3, s4, vz4, s5, vz5, s6, vz6)

# torsion diagram
plt.subplot(5, 1, 5)
plt.title('torsion')
plt.plot(s1, t1, s2, t2, s3, t3, s4, t4, s5, t5, s6, t6)

plt.show()

# easy functions for Moment, deflection and torsion (by Luc)
# Moment around z calculator in function of x

def Momenty(x):
    Moment = 0
    if x > 0 and x <= x1:
        Moment = qy / 2 * x ** 2
    if x > x1 and x <= (x2 - xa / 2):1
        Moment = qy / 2 * (x) ** 2 - R1y * (x - x1)

```

```

if x > (x2 - xa / 2) and x <= x2:
    Moment = qy / 2 * (x) ** 2 - R1y * (x - x1)
        - pry * (x - (x2 - xa / 2))
if x > x2 and x <= x2 + xa / 2:
    Moment = qy / 2 * (x) ** 2 - R1y * (x - x1)
        - pry * (x - (x2 - xa / 2)) - R2y * (x - x2)
if x > x2 + xa / 2 and x <= x3:
    Moment = qy / 2 * (x) ** 2 - R1y * (x - x1)
        - pry * (x - (x2 - xa / 2)) - R2y * (x - x2) + py * (x - (x2 + xa / 2))
if x > x3 and x <= La:
    Moment = qy / 2 * (x) ** 2 - R1y * (x - x1) - pry * (x - (x2 - xa / 2))
        - R2y * (x - x2) + py * (x - (x2 + xa / 2)) - R3y * (x - x3)
return Moment

# deflection in local y in function of x

def deflection(x):
    deflection = 0
    if x > 0 and x <= x1:
        deflection = -(qy / 24. * x ** 4 + c1 * x + c2) / (E * Izz)
    if x > x1 and x <= (x2 - xa / 2):
        deflection = -(qy / 24. * x ** 4 + c1 * x + c2
            - R1y * (x - x1) ** 3 / 6) / (E * Izz)
    if x > (x2 - xa / 2) and x <= x2:
        deflection = -(qy / 24. * x ** 4 + c1 * x + c2 - R1y * (x - x1) ** 3 / 6
            - pry * (x - (x2 - xa / 2)) ** 3 / 6) / (E * Izz)
    if x > x2 and x <= x2 + xa / 2:
        deflection = -(qy / 24. * x ** 4 + c1 * x + c2 - R1y * (x - x1) ** 3 / 6
            - pry * (x - (x2 - xa / 2)) ** 3 / 6 - R2y * (x - x2) ** 3 / 6) / (E * Izz)
    if x > x2 + xa / 2 and x <= x3:
        deflection = -(qy / 24. * x ** 4 + c1 * x + c2 - R1y * (x - x1) ** 3 / 6
            - pry * (x - (x2 - xa / 2)) ** 3 / 6 - R2y * (x - x2) ** 3 / 6
            + py * (x - (x2 + xa / 2)) ** 3 / 6) / (E * Izz)
    if x > x3 and x <= La:
        deflection = -(qy / 24. * x ** 4 + c1 * x + c2 - R1y * (x - x1) ** 3 / 6
            - pry * (x - (x2 - xa / 2)) ** 3 / 6 - R2y * (x - x2) ** 3 / 6
            + py * (x - (x2 + xa / 2)) ** 3 / 6 - R3y * (x - x3) ** 3 / 6) / (E * Izz)
    return deflection

# torsion in function of x

def torsion(x):
    torsion = 0
    if x > 0 and x <= (x2 - xa / 2):
        torsion = -qy * x * (0.25 * ca - (ca - 0.4324))
    if x > (x2 - xa / 2) and x <= (x2 + xa / 2):
        torsion = -qy * x * (0.25 * ca - (ca - 0.4324)) - pry * (ca - 0.4324)
            + prz * Ha / 2
    if x > (x2 + xa / 2) and x < La:

```

```
torsion = -qy * x * (0.25 * ca - (ca - 0.4324)) - pry * (ca - 0.4324)
           + prz * Ha / 2 + py * (ca - 0.4324) - pz * Ha / 2
return torsion

# smooth lined x and y -plot for Moment diagram.
xplot = np.arange(0, La, 0.02452)
yplot = []
ydeflection = []
torsionalongx = []
Mz = []

for i in lijst(xplot):
    yplot.append(Momenty(i))
    ydeflection.append(deflection(i))
    torsionalongx.append(torsion(i))
    Mz.append(Momenty(i))
plt.show()
print(c1,c2)
```

# Code Shear

```

1
import numpy as np
import matplotlib.pyplot as plt
from reactions_v_26Feb import torsion, VZ, VY, ydeflection,Mz
import pandas as pd

# Variables
sections = 113

# Geometric constants
la = 2.771 # m
t1 = 0.0011 # m (skin thickness)
t2 = 0.0029 # m (spar thickness)
Ca = 0.547 # m
h = 0.225 # m
G = 28e9 # N/m^2

# Calculation constants
r = h/2
A1 = (r) ** 2 * np.pi / 2
A2 = (Ca - r) * r
s1 = np.pi * r # nose part total circumference
s2 = 2 * np.sqrt(r ** 2 + (Ca - r) ** 2) # triangle part total circumference
dstr = (s1 + s2) / 17
tht2 = dstr / r
tht3 = tht2
tht1 = np.pi / 2 - tht2
tht4 = tht1
phi = np.tan(r / (Ca - r))
p_tr = np.sin(np.pi / 2 - phi) * r

#
Vz = VZ # import
Vy = VY
var = 0
T = np.zeros(sections)
Mo = np.zeros(sections)
for j in range(sections):
    T[j] = torsion(var)
    Mo[j] = torsion(var)
    var += la/(sections*1000.)

#Geometrical properties
Iyy = 5.201346425e-5 # m^4
Izz = 1.199638906e-5 # m^4

Area = np.array(

```

```

[0, 103.71, 103.71, 103.71, 103.71, 103.71, 103.71,
103.71, 182.19, 129.75, 106.83, 129.75, 182.19, 103.71, 103.71,
103.71, 103.71, 103.71, 103.71])/1000000.

zloc = np.array(
[0, 54.31, 108.62, 162.93, 217.24, 271.55, 325.86,
380.17, 434.48, 514, 547, 514, 434.48, 380.17, 325.86, 271.55,
217.24, 162.93, 108.62, 54.31])/1000.

zloc = zloc - 0.30493
yloc = np.array(
[0., -14.0625, -28.125, -42.1875, -56.25, -70.3125,
-84.375, -98.4375, -112.5, -79.55, 0., 79.55, 112.5, 98.4375,
84.375, 70.3125, 56.25, 42.1875, 28.125, 14.0625])/1000.

# Empty arrays
twist = np.zeros(sections)
qby = np.zeros(sections)
qbz = np.zeros(sections)
qb = np.zeros([20, sections])
q_shear_bend = np.zeros([20, sections])
delta_qb = np.zeros([20, sections])
# index 1 for boom 1 etc. Note: index 0 represents a nonexistent boom and is not used!
qs01 = np.zeros(sections)
qs02 = np.zeros(sections)
qsum1 = np.zeros(sections)
qsum2 = np.zeros(sections)
Vali_stress = np.zeros(sections)
VM_stresses = np.zeros([20, sections])
Ley = np.zeros(sections)
Tey = np.zeros(sections)

# Shear flows and twist due to Torque (x-axis)
for i in range(0, sections):
    eqn = np.array([[2 * A1, 2 * A2, 0], [(s1 / t1 + h / t2) / (2 * A1 * G),
    -h / (2 * A1 * G * t2), -1], [-h / (2 * A2 * G * t2),
    (s2 / t1 + h / t2) / (2 * A2 * G), -1]])
    sol = np.array([[T[i]], [0], [0]])
    x = np.linalg.solve(eqn, sol)
    twist[i] = x[2]*la/sections+twist[i-1]
    qs01[i] = x[0]
    qs02[i] = x[1]

# Calculation of 'open section' shear flows
for i in range(0, sections):
    qby[i] = -Vz[i] / Iyy
    qbz[i] = -Vy[i] / Izz
    qb[11][i] = 0.
    qb[12][i] = 0.

    for j in range(1, 20):
        delta_qb[j][i] = qby[i] * Area[j] * zloc[j] + qbz[i] * Area[j] * yloc[j]
        # jump in 'open section' shear flow at boom j

```

```

qb[10][i] = 0 + delta_qb[11][i] # These 4 lines are for cell 1
qb[9][i] = qb[10][i] + delta_qb[10][i]
qb[8][i] = qb[9][i] + delta_qb[9][i]

qb_0_II = 0 + delta_qb[12][i] # Positive downward
qb[0][i] = -qb_0_II # Positive downward

qb[7][i] = qb_0_II + delta_qb[8][i]
for j in range(8, 0, -1):
    qb[j][i] = qb[j+1][i] + delta_qb[j+1][i]

qb[19][i] = qb[1][i] + delta_qb[1][i]
for j in range(18, 12, -1):
    qb[j][i] = qb[j+1][i] + delta_qb[j+1][i]
for j in range(8, 12):
    qsum1[i] += (qb[j][i] * dstr) / t1
for j in range(1, 8):
    qsum2[i] += 2 * (qb[j][i] * dstr) / t1
for j in range(12, 20):
    qsum2[i] += 2 * (qb[j][i] * dstr) / t1

# Deflection due to shear
for i in range(0, sections):
    Mo_nose_qb = qb[11][i] * r ** 2 * tht1 + qb[10][i] * r ** 2 * tht2
    + qb[9][i] * r ** 2 * tht3 + qb[8][i] * r ** 2 * tht4
    dummy = 0
    for j in [6, 5, 4, 3, 2, 1, 19, 18, 17, 16, 15, 14, 13]:
        dummy = dummy + qb[j][i] * p_tr * dstr
    Mo_triangle_qb = qb[7][i] * p_tr * ((s2 - 13 * dstr) / 2) + dummy

    eqn = np.array([[2 * A1, 2 * A2, 0], [(s1 / t1 + h / t2) / (2 * A1),
    -h / (2 * A1 * t2), -1], [-h / (2 * A2 * t2), (h / t2 + s1 / t1) / (2 * A2), -1]])
    sol = np.array([-Mo_nose_qb - Mo_triangle_qb + Mo[i]],
    [(-qsum1[i] - qb[0][i] * h / t2) / (2 * A1 * G)],
    [(-qsum2[i] - qb[0][i] * h / t2) / (2 * A1 * G)])
    x2 = np.linalg.solve(eqn, sol)
    twist[i] += x2[2] * la.sections + twist[i - 1]

    for j in range(1, 8):
        q_shear_bend[j][i] = qb[j][i] + x2[1] + qs02[i]
    for j in range(12, 20):
        q_shear_bend[j][i] = qb[j][i] + x2[1] + qs02[i]
    for j in range(8, 12):
        q_shear_bend[j][i] = qb[j][i] + x2[0] + qs01[i]
    q_shear_bend[0][i] = (qb[0][i] + x2[0] - x2[1] + qs01[i]) # positive upward

##Deflection total
for i in range(0, sections):
    Ley[i] = -np.sin(twist[i]) * r - ydeflection[i]
    Tey[i] = np.sin(twist[i]) * (Ca - r) - ydeflection[i]

```

```
#Von Mises stresses
for i in range(sections):
    for j in range(20):
        VM_stresses[j,i] = abs(q_shear_bend[j,i]/dstr)+Mz[i]*yloc[j]/Izz

#VM stress from Reinier
name = "LC1"
filenameInput = 'A320_Comp_'+name+'.csv'

df = pd.read_csv(filenameInput)
print()
print("//Imported data")

headers = list(df.columns.values)
dataset = {}

flag = 0
for header in headers:
    dfToList = df[header].tolist()
    dfList = list(df[header])
    if flag>0:
        dataset[header]=dfList
    flag = flag + 1

for i in range(sections):
    Vali_stress[i] = dataset["MiseStress"][9+19*i]
    if dataset["MiseStress"][9+19*i] == 0.0 :
        Vali_stress[i] = Vali_stress[i-1]

# Plotting shear flows
im = plt.imread("Figure2.png")
implot = plt.imshow(im)
y = [265, 340, 350, 360, 370, 380, 390, 390, 380, 310,
     230, 160, 140, 140, 150, 160, 170, 180, 190, 200]
z = [210, 570, 510, 450, 390, 330, 270, 210, 150, 100,
     90, 130, 190, 250, 310, 370, 430, 490, 550, 650]
for i in range(20):
    plt.annotate(round(q_shear_bend[i, 56],2), (z[i], y[i])) # adjust to choose slice
plt.xlabel("z")
plt.ylabel("y")
plt.title("Shear flows")
plt.show()

#Plotting Von Mises Stresses
plt.title("Von Mises stresses")
plt.ylabel('$\sigma$[MPa]')
plt.xlabel("span")
plt.plot(VM_stresses[9], label = "Numerical")
plt.plot(Vali_stress,label = 'Finite Element')
plt.legend()
```

```
plt.show()

#Plotting Twist
plt.title("twist")
plt.ylabel("angle")
plt.xlabel("sections")
plt.plot(twist)
plt.show()
```

## ORIGINALITY REPORT



### PRIMARY SOURCES

- |          |  |               |
|----------|--|---------------|
| <b>1</b> | <b>Submitted to Technische Universiteit Delft</b><br>Student Paper   | <b>10%</b>    |
| <b>2</b> | H. Toetenel, R.L. Spelberg, S. Stuurman, J. van Katwijk. "Modeling and analysis of complex computer systems-the MTCCS approach", Proceedings of ICECCS '96: 2nd IEEE International Conference on Engineering of Complex Computer Systems (held jointly with 6th CSESAW and 4th IEEE RTAW), 1996<br>Publication | <b>1%</b>     |
| <b>3</b> | <b>Submitted to Middlesex University</b><br>Student Paper  | <b>1%</b>     |
| <b>4</b> | Aquilano, D.. "Theoretical equilibrium and growth morphology of anhydrite ( $\text{CaSO}_4^4$ ) crystals", Journal of Crystal Growth, 199212<br>Publication  | <b>&lt;1%</b> |
| <b>5</b> | <b>epdf.tips</b><br>Internet Source  | <b>&lt;1%</b> |
| <b>6</b> | Karlstrom, A.. "Efficiency of trenches along railways for trains moving at sub- or supersonic  | <b>&lt;1%</b> |

speeds", Soil Dynamics and Earthquake Engineering, 200707

Publication

- 7 D.L. McWilliams. "Simulation-Based Scheduling for Parcel Consolidation Terminals: A Comparison of Iterative Improvement and Simulated Annealing", Proceedings of the Winter Simulation Conference, 2005., 2005

Publication

<1 %

- 8 Ben Niu, Huan Li, Tian Qin, Hamid Reza Karimi. "Adaptive NN Dynamic Surface Controller Design for Nonlinear Pure-Feedback Switched Systems With Time-Delays and Quantized Input", IEEE Transactions on Systems, Man, and Cybernetics: Systems, 2018

Publication

<1 %

- 9 Submitted to Imperial College of Science, Technology and Medicine

Student Paper

<1 %

- 10 [www.komite.net](http://www.komite.net)

Internet Source

<1 %

- 11 Submitted to University of Edinburgh

Student Paper

<1 %

- 12 [gitlab.lif.univ-mrs.fr](https://gitlab.lif.univ-mrs.fr)

Internet Source

<1 %

- 13 [repository.up.ac.za](https://repository.up.ac.za)

<1 %

14

[www.ccamlr.org](http://www.ccamlr.org)

Internet Source

<1 %

15

"Two-Dimensional Incompressible Laminar Flows", Modeling and Computation of Boundary-Layer Flows, 2005

Publication

<1 %

16

[repository.ntu.edu.sg](http://repository.ntu.edu.sg)

Internet Source

<1 %

17

Submitted to Manchester Metropolitan University

Student Paper

<1 %

18

Johan Holmgren. "Prediction of tree height, basal area and stem volume in forest stands using airborne laser scanning", Scandinavian Journal of Forest Research, 12/1/2004

Publication

<1 %

19

Fundamentals of Biomechanics, 1999.

Publication

<1 %

20

[hal.archives-ouvertes.fr](http://hal.archives-ouvertes.fr)

Internet Source

<1 %

21

"Complex Job-Shop Scheduling", GOR Publications, 2006

Publication

<1 %

- 22 Todoroki, Y.. "Ring conformational requirement for biological activity of abscisic acid probed by the cyclopropane analogues", *Tetrahedron*, 19960610 <1 %  
Publication
- 
- 23 [www.sachverstaendigenrat-wirtschaft.de](http://www.sachverstaendigenrat-wirtschaft.de) <1 %  
Internet Source
- 
- 24 [www.ncgeo.nl](http://www.ncgeo.nl) <1 %  
Internet Source
- 
- 25 E. Berggren. "Rotational diffusion of biaxial probes in biaxial liquid crystal phases", *Molecular Physics*, 6/10/1995 <1 %  
Publication
- 
- 26 A.H. Mueller, A.I. Shoshi. "Small-x physics beyond the Kovchegov equation", *Nuclear Physics B*, 2004 <1 %  
Publication
- 
- 27 [etd.lib.metu.edu.tr](http://etd.lib.metu.edu.tr) <1 %  
Internet Source
- 
- 28 Pulla, Devi Prasad, and Albert Conlisk. "A Lifting Surface Study of Helicopter Aerodynamics in Ground Effect", 45th AIAA Aerospace Sciences Meeting and Exhibit, 2007. <1 %  
Publication
- 
- 29 Qingzhen Xu. "M x / G /1 Queue with Multiple Vacations", *Stochastic Analysis and* <1 %

# Applications, 1/1/2007

Publication

---

Exclude quotes Off

Exclude bibliography Off

Exclude matches Off

FINAL GRADE

GENERAL COMMENTS

### Instructor

# 53 /100

---

PAGE 1

---

PAGE 2



**Comment 1** | Re. overview

Overall good report structure, with some minor grammatical errors.

---

PAGE 3



**Comment 2** | Re. overview

Clear introduction.

---

PAGE 4



**Comment 3** | Num. model

Good general assumptions and effects discussed, however some secondary effects are missing. For e.g. neglecting of twist-induced bending at the hinge line, taking small angle approximation etc.



**Comment 4** | Num. model

Good that you checked this



**Comment 5** | Num. model

What is the effect of making this assumption?

---

PAGE 5



## Comment 6 | Re. overview

Reference?

PAGE 6

---



## Comment 7 | Analyt. model

Although the assumptions are well outlined, the description of the method is quite brief. Aspects that are missing are: a check on the correctness of the model and a good motivation for why the given model is valid to verify your results with.



## Comment 8 | Analyt. model

Good that you identified these assumptions/mistakes. However, effects of the assumptions which you did not modify (other than the centroid on hingeline) were not discussed.



## Comment 9 | Analyt. model

This isn't the only reason by the load cases can be superimposed (linear problem!).



## Comment 10 | Analyt. model

Correct



## Comment 11 | Analyt. model

Very good that you did this, but it was not necessary. In any case, this type of discussion when you're comparing the results of the analytical and numerical models belong in the verification chapter.



## Comment 12 | Analyt. model

The description of the analytical model and the underlying theory could have been more elaborate. Furthermore, a checks for correctness are missing.

PAGE 7

---

PAGE 8

---



## Comment 13 | Num. model

Relevant numerical model used with some mistakes. An explicit analysis of how you determine the shear stress in the ribs is also missing.



## Comment 14 | Num. model

Reference?

**Comment 15** | Num. model

Some secondary assumptions are missing.

PAGE 9

---

**Comment 16** | Num. model

Correct

**Comment 17** | Num. model

Good that you checked this.

**Comment 18** | Num. model

Not clear how you account for varying stress ratios along the span of the aileron and subsequently varying boom areas.

**Comment 19** | Num. model

You do not take into account that bending is unsymmetrical. The neutral axis would not remain the same.

**Comment 20** | Num. model

How? You should be more specific.

PAGE 10

---

PAGE 11

---

PAGE 12

---

**Comment 21** | Num. model

Correct approach.

PAGE 13

---

**Comment 22** | Num. model

Nice and clear FBD.

PAGE 14

---



## Comment 23 | Re. overview

Reference?

PAGE 15

---

PAGE 16

---



## Comment 24 | Num. model

No explanation of how Von-mises stresses are computed.



## Comment 25 | Num. model

How did you decide on this?

PAGE 17

---



## Comment 26 | Num. model

Good clear pseudocode and flowchart.

PAGE 18

---

PAGE 19

---



## Comment 27 | Verification

A good overview of the comparison between the analytical model and the numerical model is provided with discussion on the source of discrepancies. However, very limited independent tests are proposed



## Comment 28 | Verification

The numerical model is only compared with the analytical model and no independent testing is done.

Section 5.1 could have been more detailed with unit tests done to verify the model independently as well.

PAGE 20

---



## Comment 29 | Verification

Good analysis.



## Comment 30 | Verification

Clearly presented data, gives good overview of your results.



**Comment 31 |** Verification

Good



**Comment 32 |** Verification

Good description, but a more thorough quantitative analysis is required with regard to evaluating discrepancies.



**Comment 33 |** Verification

Twist distribution verification not presented.



**Comment 34 |** Verification

Tests do not cover the entire model.



**Comment 35 |** Validation

The validation data is well explained, however the one comparison made is incorrect and the section is missing more validation tests. Furthermore, accuracy of the numerical model as compared to the data provided was not arrived at.



**Comment 36 |** Validation

Correct simplification, but a more detailed description of how you arrived at this would have been nice. Especially since you're using a structural idealisation with boom, where will you be determining the VM stresses? Since the skin and booms only carry shear and normal stresses respectively, there is no point on your cross section that combines all the stresses that are used for the VM equation. How would you have gotten around that?



**Comment 37 |** Validation

Very contradictory sentences.



**Comment 38 |** Validation

Unlikely, it would have been better to go back over your program and methodology to find the

UNLIKELY, IT WOULD HAVE BEEN BETTER TO GO BACK OVER YOUR PROGRAM AND METHODOLOGY TO FIND THE ERROR SOURCES.



## Comment 39 | Validation

A good first step, but a quantitative error analysis is missing! It's important to quantify the differences in your validation process and try to pinpoint the error sources if possible.

---

PAGE 26

---

PAGE 27

---

PAGE 28

---

PAGE 29

---

PAGE 30

---

PAGE 31

---

PAGE 32

---

PAGE 33

---

PAGE 34

---

PAGE 35

---

PAGE 36

---

PAGE 37

---

PAGE 38

---

PAGE 39

## RE. OVERVIEW (5%)

75 / 100

SCALE 1 (0)	Task division is missing
SCALE 2 (20)	
SCALE 3 (40)	Report is not structured Many incorrect sentences Task division incomplete
SCALE 4 (50)	
SCALE 5 (60)	Structure sufficient Several spelling and grammatical errors Task division present, but needs revision
SCALE 6 (65)	
SCALE 7 (70)	Good structure Minor and spelling and grammatical errors Clear task division present
SCALE 8 (75)	
SCALE 9 (80)	Good structure and layout, references included Few spelling and grammatical errors
SCALE 10 (90)	
SCALE 11 (100)	Very good structure and layout, textbook style, including referencing No spelling and grammatical errors

## ANALYT. MODEL (15%)

60 / 100

SCALE 1 (0)	Description of method missing Results missing Assumptions missing Equations missing
SCALE 2 (20)	
SCALE 3 (40)	Description of method partly missing or contains mistakes Provided model not tested Results missing or with large mistakes that are not explained Missing important assumptions Effects of assumptions missing or wrong
SCALE 4 (50)	
SCALE 5	Description of method contains small mistakes and no or wrong motivation for why

(60)	this is a good model to verify the numerical model Test done to see if the provided model is correct Results have mistakes, explanation given for deviations Contains the most important assumptions Effort is made to show effects of assumptions but no explanation how these effects are obtained
SCALE 6 (65)	
SCALE 7 (70)	Description of method correct and some motivation is given why this is a good model to verify the numerical model Multile tests done to see if the provided model is correct Results with small mistakes which are explained Most of the important and secondary assumptions and their effects given (where possible), little explanation how these effects are obtained
SCALE 8 (75)	
SCALE 9 (80)	Good description of the method and good motivation for why this is a good model to verify the numerical model Explanation which tests for correctness of the provided model are done and why the provided model is correct Results are correct Most important and secondary assumptions and their effects given (where possible) and explanation how these effects are obtained.
SCALE 10 (90)	
SCALE 11 (100)	Clear, unambiguous description of the method, and motivation as in a textbook for why this is a good model to verify the numerical model. Excellent explanation how the provided model is tested and discussion how it is concluded that the model is correct All assumptions described, creativity shown in describing their effects (where possible).

#### NUM. MODEL (30%)

60 / 100

SCALE 1 (0)	Assumptions and effects missing Equations missing Method missing No results given
SCALE 2 (20)	
SCALE 3 (40)	Missing all main assumptions or wrong assumptions mentioned Effects of main assumptions partly missing or wrong Irrelevant numerical method used or mistakes in equations used Results do not make sense, no explanation
SCALE 4 (50)	
SCALE 5 (60)	A few main assumptions are given Effects of assumptions are given, but no motivation of their possible effect on results Relevant numerical method used, but some mistakes in or missing description Results have mistakes which are addressed
SCALE 6	

(65)

SCALE 7

(70)

Main assumptions are given Effects of main assumptions is described (where possible) Relevant numerical method used, with some motivation Results have small mistakes which are sufficiently addressed

SCALE 8

(75)

SCALE 9

(80)

Assumptions are complete Effects of assumptions are described (where possible) Motivation for the effects on results is given Relevant numerical method used, no mistakes made and with good motivation Results are correct

SCALE 10

(90)

SCALE 11

(100)

All assumptions that can be expected Effect on results and motivation show creativity beyond what can be expected. Numerical method is tailored to reach high accuracy.

**VERIFICATION (25%)**

70 / 100

---

SCALE 1

(0)

No unit tests No larger (system) tests No motivation for why these tests are sufficient. No description of the accuracy of the tests

SCALE 2

(20)

SCALE 3

(40)

One unit test performed and described Larger (system) test wrong or incomplete No motivation for why these tests are sufficient

SCALE 4

(50)

SCALE 5

(60)

Several unit tests performed, but with mistakes, Results reported larger (system) test relevant but with mistakes, results reported Tests do not cover the entire model. Accuracy of at least one test given.

SCALE 6

(65)

SCALE 7

(70)

Several unit tests performed Results reported, effort made to show what is done with test results Larger (system) test relevant Results reported Accuracy of tests given, but with mistakes Tests cover most of the entire model but this is not demonstrated.

SCALE 8

(75)

SCALE 9

(80)

Several unit tests are performed larger (system) tests relevant and motivated. Results are described, it is mentioned what action is taken based on test result (if applicable) Accuracy of tests given with some motivation Effort is made to show that tests cover the entire model

SCALE 10  
(90)

SCALE 11  
(100) Unit tests good, creativity shown in finding tests larger tests are relevant, creativity shown in designing tests Excellent description of results of tests and actions taken (if applicable). Accuracy of tests given and motivated Tests are shown to cover the entire model

**VALIDATION (25%)**

20 / 100

---

SCALE 1  
(0) Validation missing

SCALE 2  
(20)

SCALE 3  
(40) Validation tests wrong or incomplete Discrepancies wrongly addressed or explained

SCALE 4  
(50)

SCALE 5  
(60) Validation tests sufficient, but with some errors or missing description Effort is made to address or explain discrepancies, some mistakes

SCALE 6  
(65)

SCALE 7  
(70) Validation more than sufficient, room for improvement in description Discrepancies sufficiently addressed or explained. Effort is made to relate them to assumptions or accuracy in model and data.

SCALE 8  
(75)

SCALE 9  
(80) Validation test, well described Discrepancies are addressed or explained and related to assumptions or accuracy in model and data.

SCALE 10  
(90)

SCALE 11  
(100) validation tests good, creativity shown, very well described. Discrepancies are assessed fully consistently with description of assumptions and their effects, and the uncertainty in validation data